THE ASTROPHYSICAL JOURNAL, 329:629–640, 1988 June 15

LONG-SLIT SPECTROSCOPY OF STARBURST GALAXIES[1]

M. M. DE ROBERTIS[2, 3] AND RICHARD A. SHAW
Lick Observatory, Board of Studies in Astronomy and Astrophysics
Received 1987 September 30; accepted 1987 December 8

ABSTRACT

We present high-resolution, long-slit spectra of nine optically bright nuclear starburst galaxies (SBGs) selected from the sample of Balzano from which we measure line strengths, line widths, and velocity profiles along the slit in the Hα, [N II], and [S II] emission lines. We show that these galaxies have strong nebular emission (and presumably star formation) extending over several hundred to more than 1000 pc from their centers. We find that the peak of the continuum and line emission profiles are displaced from the center (as defined by the rotation curve) in many of the galaxies. Gas densities and ionization levels in the SBGs fall in the range expected for giant H II region complexes, although the line widths are often much larger.

The velocity profile in each galaxy is consistent with a rotation curve in which emission-line material is confined to a disk coaligned with that of the parent galaxy. The starburst must therefore consist of from tens to thousands of massive H II regions rather than one giant, spherical complex. The line widths would then result from an intrinsic velocity dispersion and rotational broadening.

Although SBGs and active galaxies occur in similar environments and have similar space densities, we find little similarity (spectroscopically or morphologically), nor any direct evidence for an evolutionary link between them. Time scale arguments suggest that if such a link does exist, then the active galaxy phase must succeed the SBG phase, although probably not in the manner suggested by Weedman.

Subject headings: galaxies: internal motions — galaxies: nuclei

I. INTRODUCTION

Since they were first examined as a class, "starburst" galaxies (hereafter SBGs) have attracted much attention as galaxies with intense nuclear activity and as possible precursors of active galactic nuclei (hereafter AGNs) (see e.g., Weedman *et al.* 1981; Feldman *et al.* 1982; Balzano 1983; Weedman 1983). Indeed, many similarities have been reported. Balzano (1983) has noted that about 30% of SBGs apparently have companion galaxies, similar to that found for AGNs by Dahari (1984)—i.e., a significantly higher rate than for normal galaxies. As well, Weedman (1983) pointed out that the space density for optically bright SBGs is roughly the same as for Seyfert galaxies. Several authors have found prominent star formation activity surrounding the nuclei of Seyfert 1 galaxies (e.g., De Robertis and Pogge 1986; Wilson *et al.* 1986) and Seyfert 2 galaxies (e.g., Telesco *et al.* 1984); and Feldman *et al.* (1982), and Taniguchi (1987) have published line widths for some SBGs which approach those found in the narrowest width AGNs (see, e.g. Phillips, Charles, and Baldwin 1983; Whittle 1985). It is well known that the continuum source and line-emitting regions in AGNs occupy a volume much less than ~200 pc in diameter, and probably less than 10 pc. The spatial extent of star formation in SBGs has not been well studied, however. According to Balzano (1983), the most dominant morphological feature of SBGs, as for AGNs, is a bright star-like nucleus. But unlike AGNs, the low-ionization, narrow emission lines in SBGs can be produced by the thermal continuum of hot, young stars (Evans and Dopita 1985) and does not require a photoionizing spectrum extending to high energy, often characterized by a power law.

Compared with AGNs, very little high-quality, long-slit spectroscopy is available for SBGs. Most of the published spectra were taken by Balzano (1983) and Feldman *et al.* (1982) using a Vidicon with a one-dimensional readout. In an effort to study these galaxies using present-day detectors capable of high spatial and wavelength resolution and to examine possible connections between SBGs and AGNs, we have observed several SBGs selected from Balzano's (1983) survey, based on their availability and brightness, including the prototype, NGC 7714 (Weedman *et al.* 1981). We wished to analyze several properties, including the kinematics of the emission-line material through the measurement of line widths, intensity and line profiles, and radial velocity profiles. Toward this end, we obtained high-resolution, long-slit CCD spectra of nine SBGs in the (redshifted) Hα region with a high signal-to noise ratio. In § II we present the observational details of our program and describe the analysis in § III. A discussion of the individual objects is given in § IV, and in § V we summarize our findings and discuss the implications for the starburst phenomenon and possible evolutionary links between SBGs and AGNs.

II. OBSERVATIONS

We observed eight galaxies at the coudé focus of the 3 m Shane telescope of Lick Observatory on 1986 October 5 UT, using a TI 800 × 800 three-phase CCD detector (Lauer *et al.* 1984). The galaxy NGC 2512 was observed at the Cassegrain focus of the 1.83 m telescope at the Dominion Astrophysical Observatory on 1987 March 29 UT, using a 640 × 1024 RCA CCD. The observing summary for these observations is presented in Table 1. We list, in order, the common catalog name, the exposure time, and the range of position angles of the slit for each spectrum. For the Lick data, the slit was oriented N-S on the meridian, but since we did not use an image rotator, the slit position angle changed with hour angle; the average posi-

[1] Lick Observatory Bulletin, No. 1094.
[2] Now at Department of Physics, York University, Toronto, Ontario, Canada.
[3] Guest Observer, Dominion Astrophysical Observatory, Victoria, Canada.

TABLE 1

OBSERVING SUMMARY

Galaxy	Exposure (minute)	Slit Position Angle[a]
NGC 23	40	355° ± 5°
NGC 354	60	358° ± 8°
NGC 632	60	6° ± 8°
NGC 694	60	20° ± 8°
NGC 1614	30	355° ± 4°
Mrk 1087	60	4° ± 8°
NGC 2512	48	90° ± 0°
NGC 7316	60	352° ± 8°
NGC 7714	30	351° ± 4°

[a] Includes variation during exposure.

tion and range is given in the last column in Table 1. (Because the exposure times were ~1 hr, the effects of slit rotation were negligible.) The Lick data were taken with a dispersion of 0.49 Å per pixel, with the slit opened to 430 μm, which provided a wavelength resolution of 1.0 to 1.1 Å, based upon the widths of the thorium-argon comparison lines (De Robertis and Pogge 1986). We rotated the grating to include redshifted Hα, [N II] λλ6548, 6583, and [S II] λλ6716, 6731 in each galaxy; the spectra covered about 390 Å. The spatial scale for the Lick data was 0.″4 per pixel, using a slit width of 0.″8, providing good sampling over the 1.′2 extent of the CCD. For each observation, the brightest portion of the galaxy was placed at the center of the slit. Because of the nature of the starburst, this may not coincide with the exact center of the galaxy as determined by the old stellar population (see § IV), but it is probably very close. The DAO data were binned 2 × 2 on-chip, giving a spatial scale of 0.″7 per pixel and an effective wavelength resolution of 4.5 Å.

Since line emission was apparent along much of the slit, the spectra were extracted two rows at a time from bias and flat-field corrected CCD images, and the night sky was subtracted at each column. (The spectra were sufficiently parallel to the CCD rows to make any rotational correction unnecessary. "Hot" pixels were removed using an interactive median filtering routine.) The night-sky spectrum was determined by averaging several sky rows which were centered on the rows containing the target spectra. The central row of each image was determined by measuring the centroid of the upper 50% of the continuum intensity (spatial) profile, where this profile was obtained by summing ~100 columns (i.e., along the direction of dispersion) which were free of any emission lines. As we will show below, the continuum emission is predominantly from massive young stars, and therefore the central row derived in this way may not be coincident with the center of the old stellar population of the galaxy. We fit a second-order polynomial to the sky rows on either side of the spectrum, and the appropriate interpolated sky level was subtracted from each of the spectral rows. The wavelength calibration was accomplished with the aid of thorium-argon comparison lamps taken during the night. A third-order polynomial was fitted to an average of 15 lines in each lamp, with a mean (rms) residual of 0.04 Å. Each of the target spectra were then transformed onto a linear wavelength scale using a four-point Lagrangian interpolation scheme. We corrected the spectra for atmospheric extinction using mean atmospheric coefficients for Mount Hamilton, but we did not convert intensities to energy units, owing to the narrow wavelength coverage.

III. DATA ANALYSIS

For a given object, each spectrum represents the integrated emission-line characteristics from a projected area on the sky of roughly 0.″8 × 0.″8. The adjacent spectra do not contain completely independent information, since the combined effects of seeing and guiding produced images that were approximately 1.″0 to 1.″6 in width, but they are indicative of the behavior of the emission-line material along the slit through the galaxy. Three useful parameters that can be measured from high wavelength and spatial resolution data are: the relative emission-line intensities, which describe the distribution of the emission-line material; line widths, which describe the kinematics of this material within each area, especially the velocity dispersion along the line of sight; and the relative radial velocities, which reveals the bulk behavior of matter about the galactic nucleus. Since we obtained data for each galaxy with only one slit orientation, we are not able to describe the kinematics for each nucleus in as much detail as in De Robertis and Pogge (1986), but for these purposes it is more important to study a larger number of objects.

The intensities for Hα, [N II] λ6583, and [S II] λλ6716, 6731 and full widths at half-maximum (FWHM) for Hα (and where possible [N II] λ6548) were measured in a straightforward manner as described in De Robertis and Pogge (1986). The FWHM have been corrected for finite instrumental resolution by subtracting in quadrature the mean of the widths of isolated lines in the comparison spectrum. As we shall discuss below, differential galactic rotation also contributes to line broadening. However, because the degree of the rotational component in our spectra was less than the measuring error for the FWHM (even for the most extreme case, NGC 23), and because any correction would be somewhat model dependent, we preferred not to correct this effect.

The relative velocities were measured using a cross-correlation technique: the spectrum representing the central row for each galaxy was used as a zero point against which the other emission-line spectra were correlated; the cross-correlation was carried out in the real domain. Briefly, the spectra were first placed on a linear-logarithmic scale with the mean continuum value subtracted and then Fourier filtered to remove unwanted high and low frequencies before cross-correlating. The centers of the cross-correlation peaks were then fitted with a second-order polynomial. In this way, the relative radial velocity of each spectrum was determined to within about 2–3 km s^{-1} for the central rows, and about 5–10 km s^{-1} for the rows furthest from the nucleus, which is higher accuracy than the method employed by De Robertis and Pogge (1986). Although the redshift for each object was initially measured from the central spectrum using an unweighted mean of the Hα and [N II] λ6583 centroids, we prefer to leave the radial velocities relative to the peak in the red continuum intensity profile (see § IV).

Table 2 contains the SBG parameters measured for each galaxy. Accompanying the name of the galaxy and its heliocentric redshift is the apparent magnitude, taken from the catalog of de Vaucouleurs, de Vaucouleurs, and Corwin (1976). The estimated inclinations of the disks of each galaxy, as measured from enlargements from the Palomar Observatory Sky Survey, is listed in the next column. Making the assumption that the projection-corrected cross section of a spiral galaxy is circular, the inclination angle can be derived from the axial ratio, b/a. Balzano (1983) provides Hβ and Hα + [N II] fluxes for all the galaxies in our sample from one-dimensional

TABLE 2

STARBURST GALAXY PARAMETERS

Galaxy	z	m_V (mag)	i	c	⟨AI20⟩	$\frac{I(\lambda6716)}{I(\lambda6731)}$	n_e (cm^{-3})	$\frac{I([S\ II])^a}{I(H\alpha)}$	$\frac{I([N\ II])^b}{I(H\alpha)}$
NGC 23	0.0153	12.8	57°	0.7	−0.08	1.12	350	0.43	0.95
NGC 354	0.0156	14.1	65	0.9	+0.06	1.20	240	0.33	0.80
NGC 632	0.0104	13.5	27	1.1	−0.13	1.17	280	0.27	0.59
NGC 694	0.0099	13.7	45	1.0	+0.13	1.20	240	0.35	0.43
NGC 1614	0.0158	13.8	51	1.6	+0.10	1.01	550	0.18	0.75
Mrk 1087	0.0278	14.8	45	0.6	+0.08	1.17	280	0.27	0.43
NGC 2512	0.0157	14.2	60	1.8	−0.01	1.05	480	0.21	0.68
NGC 7316	0.0186	13.7	10	0.8	+0.08	1.50	<100	0.26	0.55
NGC 7714	0.0093	13.1	60	0.8	+0.06	0.74	1700	0.13	0.49

[a] λλ6716+31.
[b] λλ6548+83.

Vidicon data. Although our effective slit size is different from the slit used in her measurements, we can derive a good estimate for the contribution of $F(H\alpha)$ to Balzano's $F(H\alpha + [N\ II])$ from our high-dispersion spectra. From this estimate, and Balzano's Hβ flux, we derive the average reddening in each galaxy. The extinction constant, c (the logarithmic extinction at Hβ), and the asymmetry parameter, AI20 (see Heckman *et al.* 1981) which was measured for both Hα and [N II] λ6583 from the sum of spectra within 1.″6 of the center of the galaxy along the slit, are listed in the following columns. We give the mean values of $I(\lambda6716)/I(\lambda6731)$ for the central few arcseconds (from which we derive and list the electron density in the S^+ emitting volume), and also list $I([S\ II]\ \lambda\lambda6716+6731)/I(H\alpha)$ and $I([N\ II]\ \lambda\lambda6548+6583)/I(H\alpha)$ in the next few columns. The latter two ratios were found to be approximately constant in the center of each galaxy where the data were of sufficient quality to provide a meaningful average ratio. Finally, Table 3 presents the asymmetry parameter AI20 as a function of slit position (relative to the nucleus) for three galaxies: NGC 632 (which had the largest central redward asymmetry), NGC 694 (which had the largest central blueward asymmetry), and NGC 7714 (which had a moderate amount of central blueward asymmetry). The large variation in AI20 along the slit, which we discuss in detail in § V, suggests that the reported line asymmetries in SBGs (e.g., Taniguchi 1987) do not have a straightforward interpretation.

We plot the data for each galaxy in three parts in Figures 1 through 9. The upper portions (*a*) show the intensities of [N II] and [S II], relative to that of Hα, as a function of position along the slit. (North is to the left, and south is to the right in these plots.) The Hα profile, normalized to its peak value, is plotted with solid symbols. The middle (*b*) portions show the instrumental profile-corrected velocity width (in km s^{-1}) for Hα along the slit. Finally, the lower portions (*c*) show both the measured velocity curve, expressed in km s^{-1} relative to the peak in the red continuum intensity profile, and the projection-corrected curve (see below).

TABLE 3

SPATIAL VARIATIONS OF ⟨AI20⟩

Slit Position	AI20 NGC 632	AI20 NGC 694	AI20 NGC 7714
−3.″6	+0.02	+0.00	+0.17
−2.8	−0.07	+0.01	+0.15
−2.0	−0.14	+0.10	+0.19
−1.2	−0.04	+0.08	+0.17
−0.4	−0.05	+0.15	+0.07
+0.4	−0.19	+0.14	+0.06
+1.2	−0.19	+0.08	+0.06
+2.0	−0.01	+0.06	+0.13
+2.8	+0.07	+0.04	+0.14

IV. INDIVIDUAL GALAXIES

Several of the galaxies in our sample have peculiar or noteworthy properties and are listed below in order of increasing right ascension. The term "intensity profile" refers to a spatial cut perpendicular to the dispersion through either the continuum or an emission line.

a) NGC 23 (= Mrk 545)

This is perhaps the most interesting of the SBGs in our sample. From Figure 1*a*, the core of the Hα intensity profile is slightly asymmetric, in the sense that the maximum emission occurs 1″ to 2″ outside the center defined by the continuum. The FWHM of the continuum intensity profile is about 8″ (1.76 h_{100}^{-1} kpc, where h_{100} is the Hubble constant in units of 100 km s^{-1} Mpc^{-1} throughout), while the FWHM of the Hα profile is 9.″4 (2.07 h_{100}^{-1} kpc). Since the FWHM of the point spread function is 1.″0 to 1.″6, it is clear that both the continuum- and line-emitting regions are well resolved. This is a common feature of all the galaxies in this study. In this and all other galaxies in our sample, there are no apparent stellar absorption features in the spectra, including Ca I λ6502 (Pritchet 1977). To understand the origin of the continuum, we calculated the Hα equivalent width expected if the continuum emission were nebular in origin, assuming an electron temperature of 10,000 K and a solar helium abundance. Even assuming a He^+/H^+ ratio of 0.10, the calculated Hα equivalent widths are orders of magnitude larger than those observed. Given the marked displacement of the continuum emission maximum from the center of the rotation curve, and of the closer correspondence between the peaks of the continuum and line emission, it appears that the observed continuum is from massive stars formed some distance from the galactic center in the most recent burst of star formation.

The [N II] and [S II] intensity maxima are more nearly coincident with the continuum maximum. There is a strong secondary intensity maximum in all the emission lines about 17″ to the N, about 15% as strong as the primary maximum. The FWHM and velocity profiles do not show analogous discontinuities at the same position, which suggests that there has

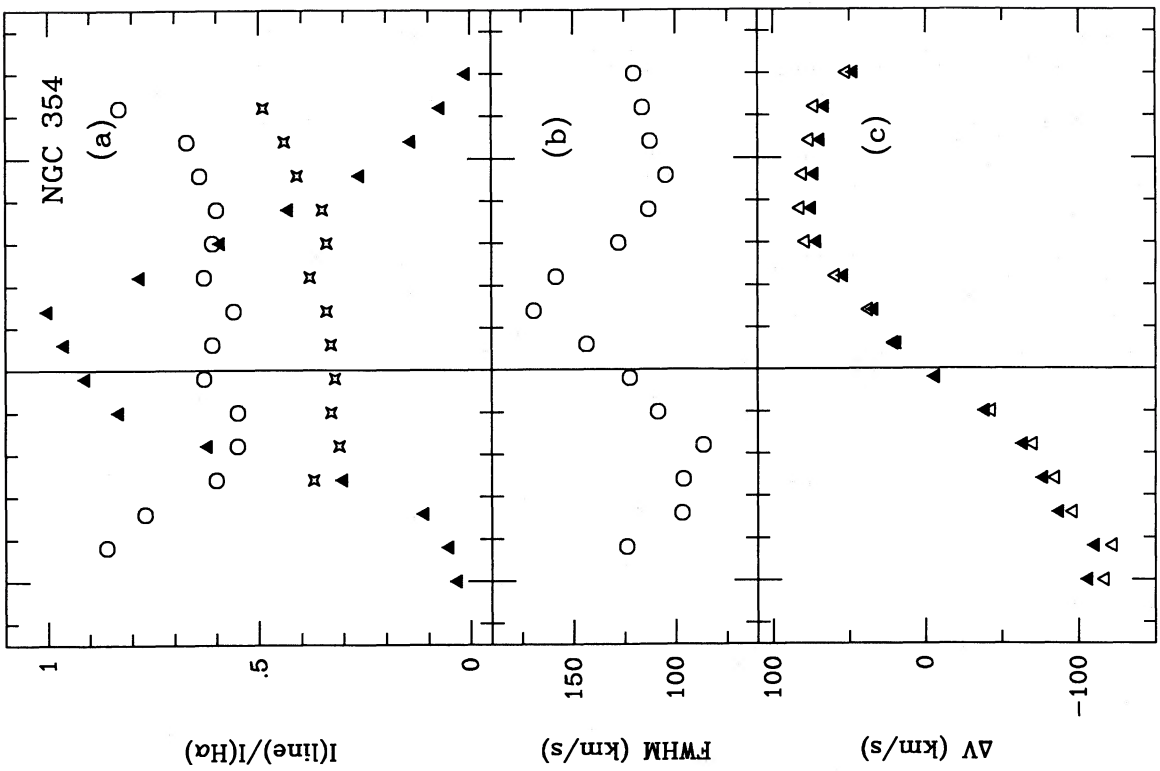

FIG. 2

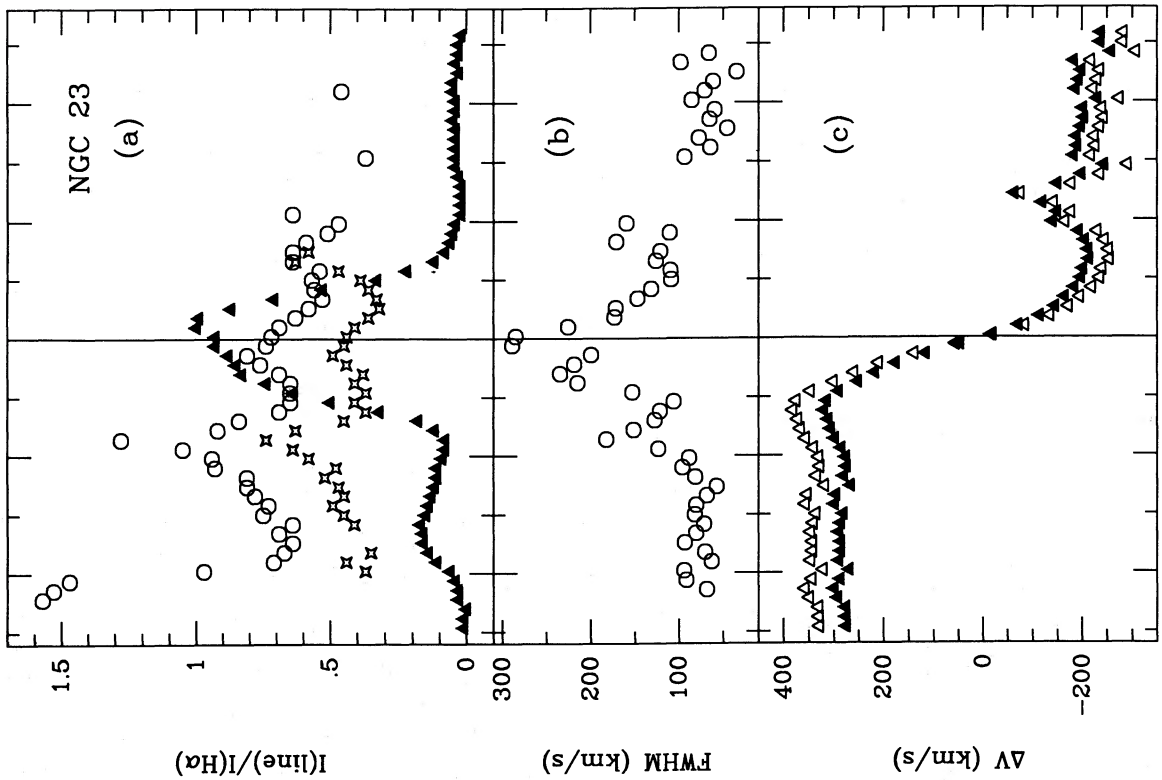

FIG. 1

FIG. 1.—(*a*) Emission-line intensities of [N II] λ6583 (*open circles*) and [S II] $\lambda\lambda$6716 + 6731 (*open stars*), relative to Hα (*filled triangles*, normalized to Hα_{max}) vs. radius in arseconds for NGC 23. North is to the left, and south is to the right. Vertical line indicates maximum in continuum emission profile: see text. (*b*) Corrected FWHM for Hα vs. radius in arcseconds for NGC 23. Vertical line as in (*a*). (*c*) Hα velocity as measured (*filled symbols*), and corrected for projection (*open symbols*), vs. radius in arcseconds for NGC 23. Vertical line as in (*a*).

FIG. 2.—(*a*) Same as Fig. 1*a*, for NGC 354. (*b*) Same as Fig. 1*b*, for NGC 354. (*c*) Same as Fig. 1*c*, for NGC 354.

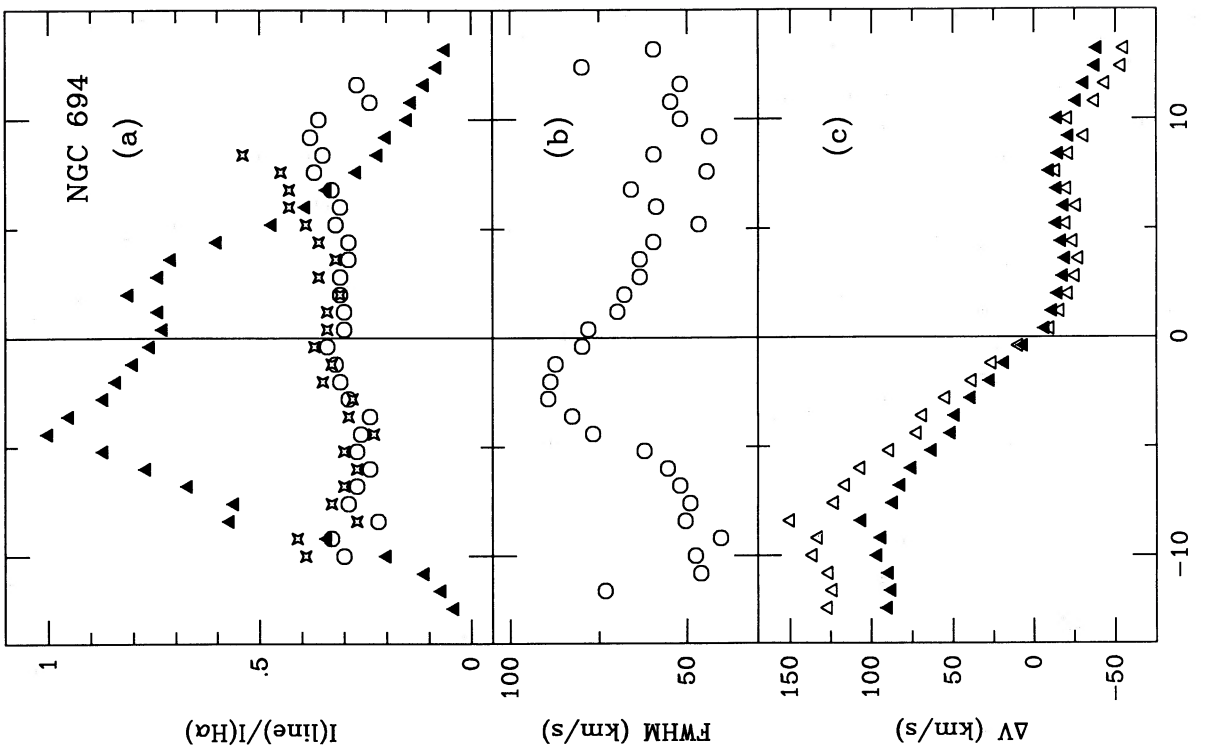

FIG. 4

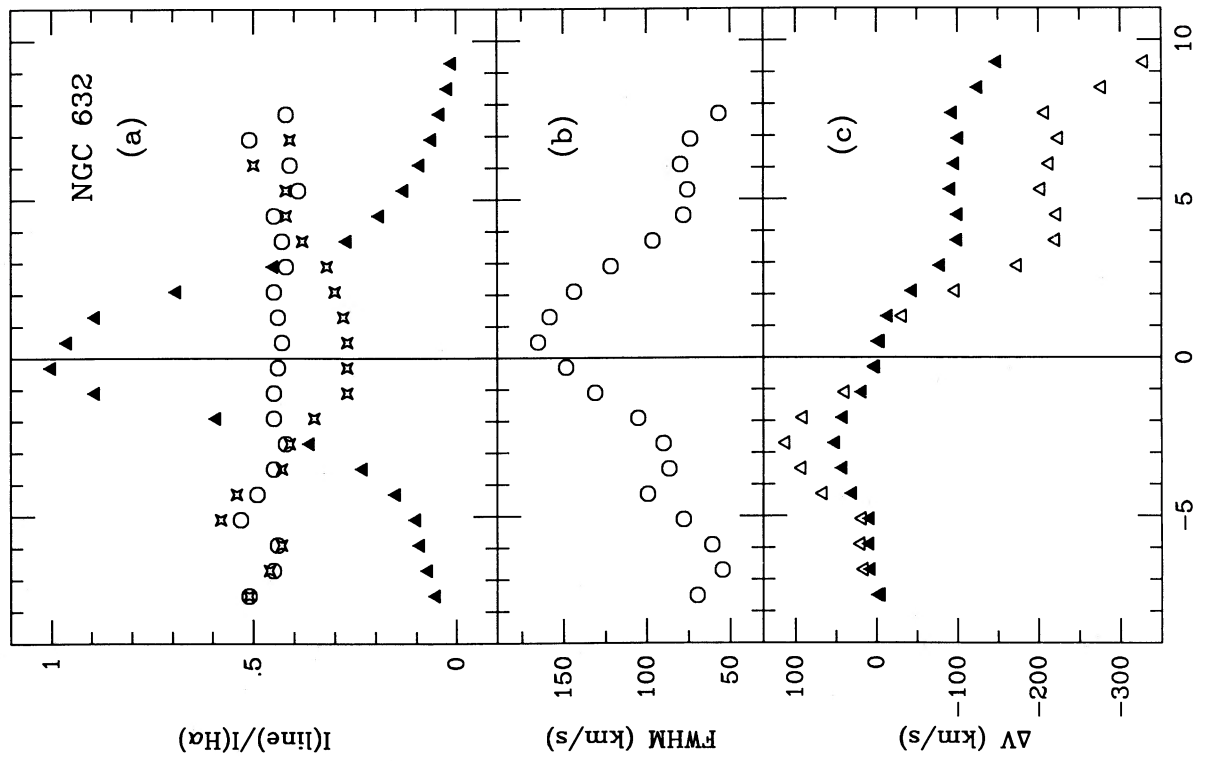

FIG. 3

FIG. 3.—(*a*) Same as Fig. 1*a*, for NGC 632. (*b*) Same as Fig. 1*b*, for NGC 632. (*c*) Same as Fig. 1*c*, for NGC 632.
FIG. 4.—(*a*) Same as Fig. 1*a*, for NGC 694. (*b*) Same as Fig. 1*b*, for NGC 694. (*c*) Same as Fig. 1*c*, for NGC 694.

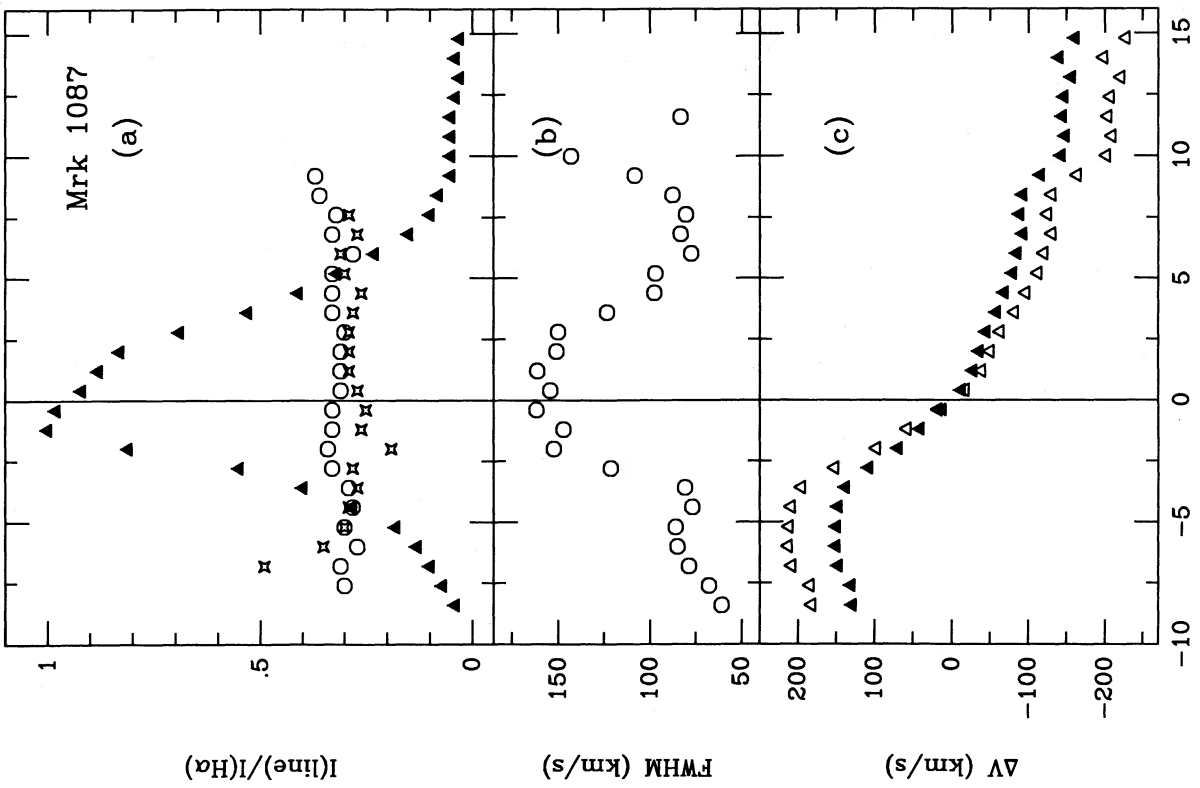

FIG. 6

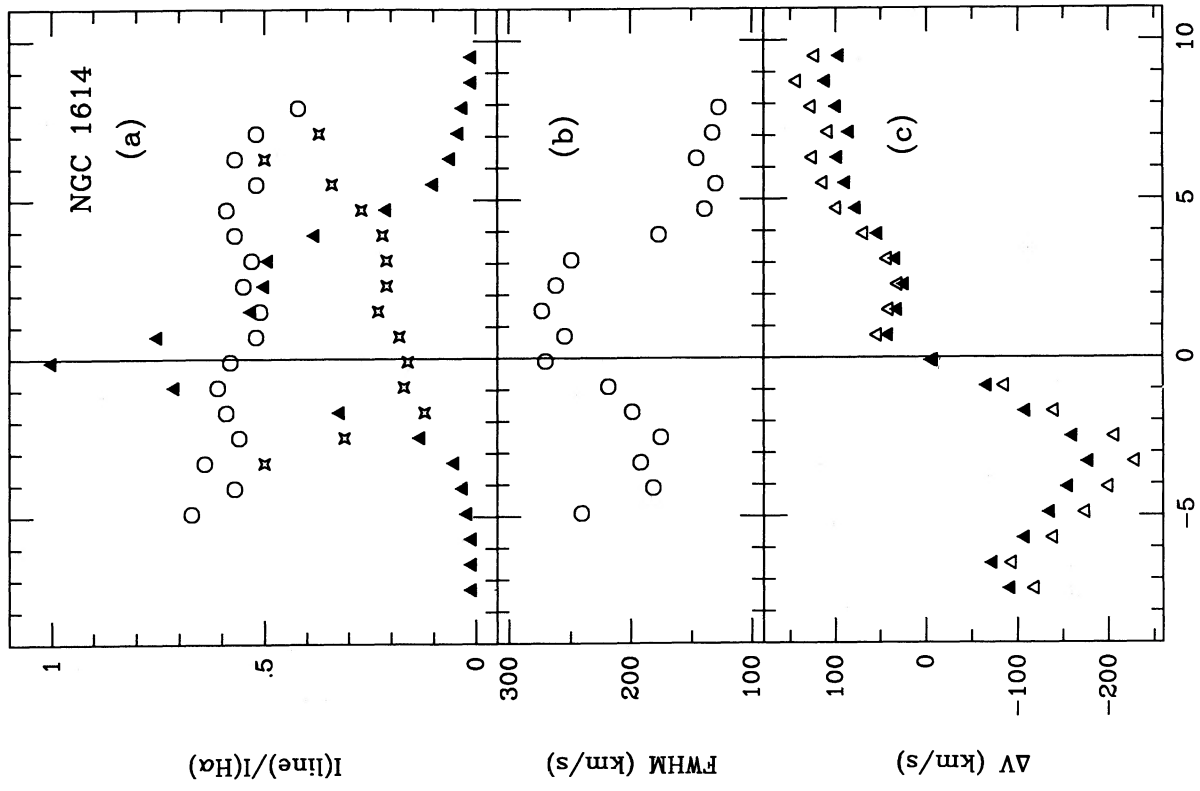

FIG. 5

FIG. 5.—(*a*) Same as Fig. 1*a*, for NGC 1614. (*b*) Same as Fig. 1*b*, for NGC 1614. (*c*) Same as Fig. 1*c*, for NGC 1614.
FIG. 6.—(*a*) Same as Fig. 1*a*, for Mrk 1087. (*b*) Same as Fig. 1*b*, for Mrk 1087. (*c*) Same as Fig. 1*c*, for Mrk 1087.

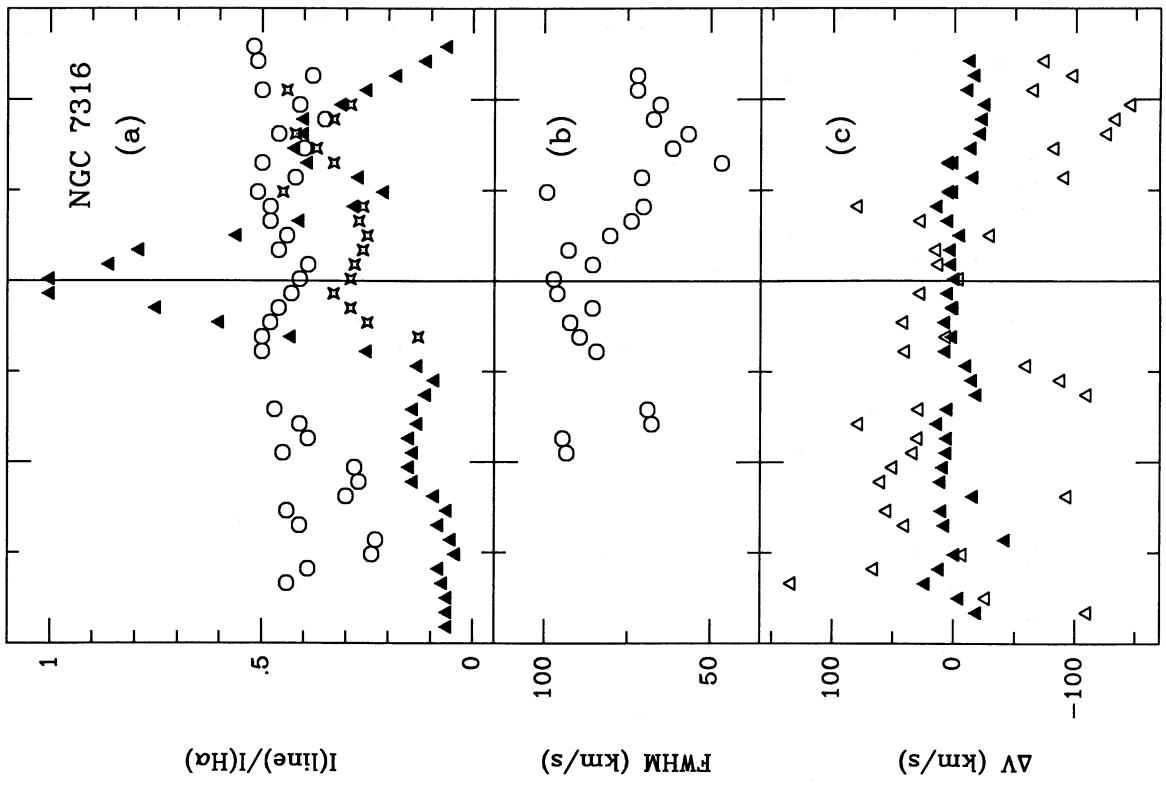

FIG. 8

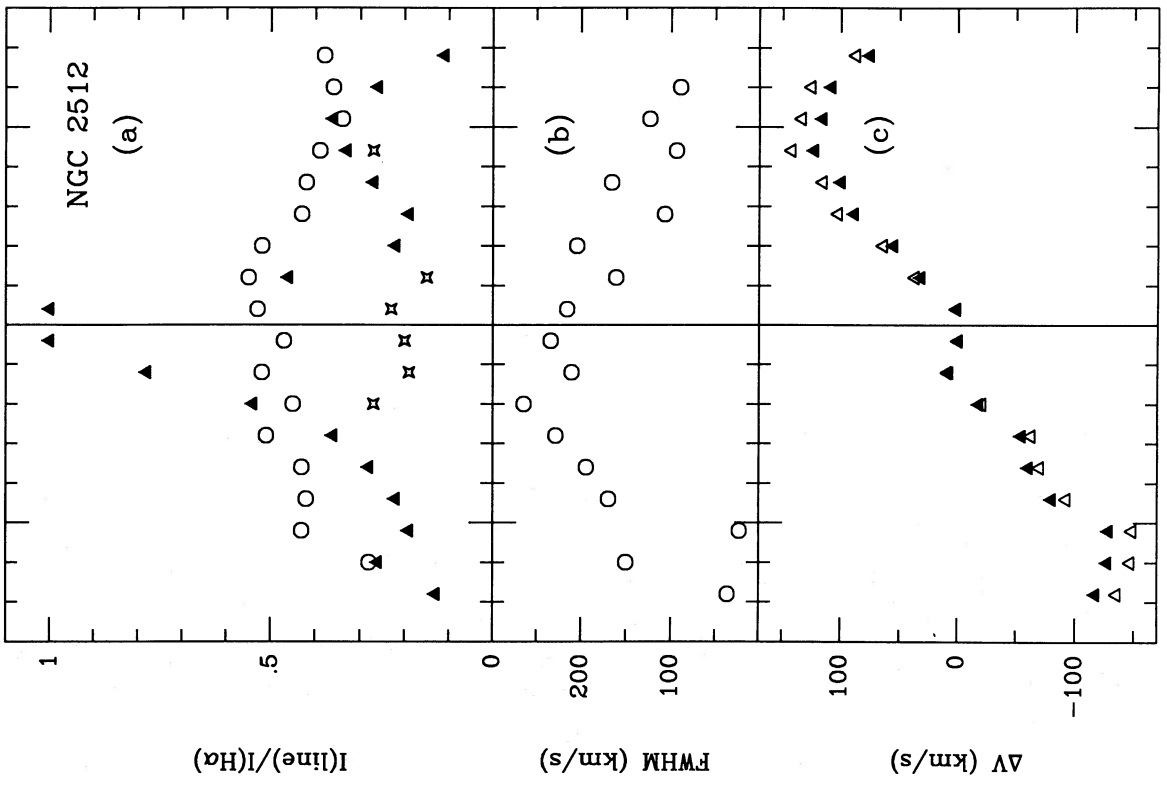

FIG. 7

FIG. 7.—(*a*) Same as Fig. 1*a*, for NGC 2512. (*b*) Same as Fig. 1*b*, for NGC 2512. (*c*) Same as Fig. 1*c*, for NGC 2512.
FIG. 8.—(*a*) Same as Fig. 1*a*, for NGC 7316. (*b*) Same as Fig. 1*b*, for NGC 7316. (*c*) Same as Fig. 1*c*, for NGC 7316.

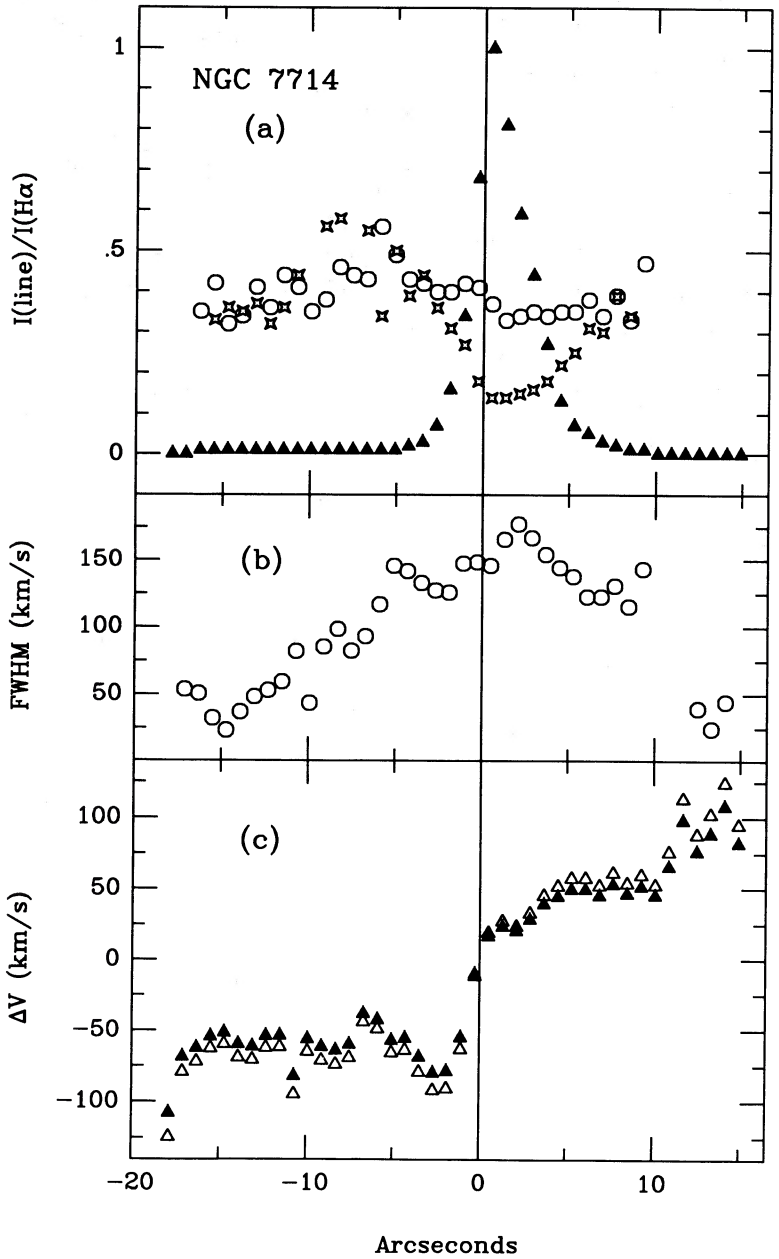

FIG. 9.—(*a*) Same as Fig. 1*a*, for NGC 7714. (*b*) Same as Fig. 1*b*, for NGC 7714. (*c*) Same as Fig. 1*c*, for NGC 7714.

been a recent burst of star formation in this volume. The FWHM profiles for Hα and [N II] differ significantly in that, while they both sharply increase toward the center, there is significantly more scatter in the Hα widths compared with the [N II] widths. The line widths in the central arcsecond approach 300 km s^{-1}—widths indicative of classical Seyferts (see e.g., Shuder and Osterbrock 1981). Is it possible that NGC 23 contains a weak AGN? The I([S II])/I(Hα) and I([N II])/I(Hα) ratios are large enough to be consistent with this suggestion, but apparently both the I([O III] λλ5007)/I(Hβ) and I([O I] λλ6300)/I(Hα) ratios (from Veilleux and Osterbrock 1987) are too small to permit NGC 23 to be classified as either a bona fide Seyfert 2 or as a LINER. Perhaps NGC 23 harbors a weak Seyfert nucleus whose spectrum is completely dominated by the H II nucleus (see § V).

The velocity profile for NGC 23 exhibits the largest amplitude of any of the galaxies in our sample. It is clear that this curve represents a rotation curve in which the emission-line material is confined to a disk. Every SBG in our sample displays similar behavior. It would be difficult to attribute velocities of this magnitude on kiloparsec scales to anything else but rotation. Thus, we will often refer to such curves as "rotation curves." Measurements from the Palomar Observatory Sky Survey (POSS) suggest that the stellar disk is inclined at 57°, and assuming the H II disk is coaligned with the stellar disk, the measured velocity amplitude of 525 km s^{-1} implies a corrected amplitude in excess of 650 km s^{-1}. Assuming that the emission-line material is in gravitational equilibrium (which appears to be reasonable, given the smoothness of the rotation curve at this position angle), then the mass interior to

2.7 h_{100}^{-1} kpc is $7 \times 10^{10}\ M_{\odot}$. NGC 23 has a very prominent western spiral arm as can be seen from the photograph in the Hubble atlas (Sandage 1961). There is an abrupt discontinuity 12″ to the S of the center of the rotation curve as can be seen in Figure 1*a*. NGC 23 does not appear to have a nearby companion galaxy as do some other SBGs in our sample.

b) NGC 354 (= Mrk 353)

This galaxy has two symmetrical spiral arms. There is no evidence for a companion galaxy or any tidal disturbance on the structure of the stellar disk itself. The intensity profiles are very interesting. The continuum profile can be deblended into two major components: a near point source with a FWHM of about 1.″9 (0.43 h_{100}^{-1} kpc), and a more extended distribution about 2.″5 (0.56 h_{100}^{-1} kpc) S of the central maximum. The emission lines have a much more extended profile, however, with a FWHM of 5.″4 (1.2 h_{100}^{-1} kpc). The maximum Hα emission occurs about 1.″5 (0.3 h_{100}^{-1} kpc) from the continuum center, while [N II] λ6583 is only slightly offset from the continuum center in the same direction. To achieve this result, the secondary component seen in the continuum profile must be almost entirely due to emission lines.

The Hα and [N II] λ6583 line widths have similar distributions. Far from the nucleus, the widths are small, but well above the instrumental FWHM of 65 km s^{-1}. There is a definite increase in line width toward the center. The maximum widths are coincident with the maximum emission-line intensities and not the center of the continuum emission. There is some evidence that the line widths reach a minimum 3″ to 4″ from the peak width and increase still further out. The rotation curve for NGC 354 is smooth, with a maximum observed velocity amplitude of 190 km s^{-1}, and an inclination-adjusted amplitude of about 210 km s^{-1}.

c) NGC 632 (= Mrk 1002)

Classified as an S0, this galaxy has an apparent companion galaxy 1.′5 or 13.5 h_{100}^{-1} kpc to the north. The continuum and emission-line intensity distributions are essentially coincident, and have FWHMs of about 5.″2, or 0.8 h_{100}^{-1} kpc. There is a slight asymmetry in all the intensity distributions in the sense that intensities fall off more quickly to the N than the S, but this effect is small. The line-width profiles of Hα and [N II] λ6583 are similar to within measuring errors, and rise to approximately ~165 km s^{-1} at the center of the galaxy.

The rotation curve is slightly unusual in that it is not symmetric about the center of the galaxy as defined by the continuum: the maximum (absolute) amplitude relative to the center in the N is 50 km s^{-1}, while in the S it is over 100 km s^{-1}. (There is some evidence that the rotation curve continues to decline outside of the region studied.) The curve reaches a maximum just to the N of the center, from which it declines at larger radii to essentially the same velocity measured for the central row. When corrected for inclination, the total velocity amplitude is over 300 km s^{-1} for NGC 632.

d) NGC 694 (= Mrk 363 = V Zw 122)

Although this compact galaxy has no visible companion associated with it, it does have an excess to the SE on the POSS. The spatial extent of the star-forming activity is dramatically shown in an image taken in the light of Hα + [N II] by Pogge and Eskridge (1987). In particular, several knots of nebular emission are apparent about 5″ to 10″ to the NW, W, and SE of the center. The emission-line intensity profiles are also highly asymmetric, even though the continuum profile is symmetric with a FWHM of 9″, or 1.3 h_{100}^{-1} kpc. There is a primary maximum in the emission-line intensity profiles: 4″ to the N, and a secondary maximum 2″ to the S. The FWHM of the emission-line intensity profiles are all greater than 14″, or 2.0 h_{100}^{-1} kpc.

The line widths are all relatively small, from just above the instrumental resolution to 85 km s^{-1}. The maximum line widths are roughly coincident with the primary maximum in the Hα emission. There is a weak indication that the [N II] FWHMs are slightly larger than for Hα. While the rotation curve for NGC 694 appears smooth and continuous, it is not symmetric about the center of the continuum emission. The rotation curve is, however, symmetric about a point 2.″4 (0.35 h_{100}^{-1} kpc) to the N, which is close to the primary maximum of the emission-line intensities. It appears then that the center of the galaxy is better represented by the center of the emission-line intensity profiles than the continuum profile. The maximum observed velocity amplitude is 130 km s^{-1}, or 180 km s^{-1} when corrected for inclination. There is also some indication that the rotation curve on the S side of the galaxy declines even further outside the largest measured radii.

e) NGC 1614 (= Mrk 617 = II Zw 15)

The "fuzz" about NGC 1614 is highly asymmetric, suggesting a recent tidal interaction between this and another galaxy. The only galaxy in the vicinity on the POSS is considerably smaller than NGC 1614, about 5′ to the SE. The continuum and emission-line intensity profiles are very similar, with a sharp primary maximum having a FWHM of 2.″4 (or 0.55 h_{100}^{-1} kpc), and a secondary maximum, about 15% the intensity of the central maximum, located about 3″ (or 0.64 h_{100}^{-1} kpc) to the S.

The line widths are rather broad compared with most of the other SBGs, with Hα and [N II] λ6583 having widths of 270 km s^{-1} near the center of the galaxy. In fact, the maximum line widths occur over a large range in radii to the S of the center of the galaxy (i.e., to the same side as the intensity excesses). Outside this plateau there is a steady decline in line widths to about 150 km s^{-1}. The rotation curve for NGC 1614 is asymmetric, with a very sharp minimum about 3.″2 to the N, and an excess to the S of the nucleus coincident with the other measured quantities. The curve is flat at large radii to the S, but rises sharply from a minimum to the N. The total measured velocity amplitude for this galaxy is 210 km s^{-1}. The image of NGC 1614 is highly asymmetric on the POSS, so there is a large uncertainty in the inclination. Using the adopted inclination of 51°, the corrected amplitude is 275 km s^{-1}.

f) Mrk 1087 (= II Zw 23)

The "fuzz" about this galaxy is highly asymmetric on the POSS, with nonstellar extensions to the S and NE. There is a galaxy of comparable luminosity about 1.′5 or 36 h_{100}^{-1} kpc to the SW. The continuum and intensity profiles are similar and symmetric to first order, except that the intensity maxima are around 1″ to the N of the center of the galaxy. There is a slight excess of continuum light throughout the S of Mrk 1087. The FWHM of the intensity profiles is about 6.″6, or 2.65 h_{100}^{-1} kpc.

The FWHM distributions for Hα and [N II] λ6583 follow a pattern similar to the intensities in that there is a maximum line width of about 170 km s^{-1} in the central region, falling to a few tens of km s^{-1} in the outer radii; the decline is slower to the S. The rotation curve is slightly asymmetric, with a shal-

lower slope to the S of the nucleus, the same direction as the other excesses. The maximum observed velocity amplitude is about 300 km s^{-1}, or when corrected for inclination, 415 km s^{-1}. On the N side there is a clear maximum 5″ to 6″ from the central row, while on the S side there is a prominent dip in the curve about 8″ from the center. There is some indication that the minimum velocity has not yet been reached, although the rotation curve levels off beyond 10″, or 4 h_{100}^{-1} kpc.

g) NGC 2512 (= Mrk 384)

NGC 2512 is a two-armed spiral with no evidence for a nearby companion galaxy. There appear to be one or two giant H II regions approximately 25″ to 30″ (5.8 to 6.9 h_{100}^{-1} kpc) from the nucleus. The continuum and emission lines have similar intensity profiles with FWHMs of 2.″5, or 0.6 h_{100}^{-1} kpc. That is, the continuum and line emission are resolved, although they are very centrally concentrated. There is a secondary maximum in both the continuum and emission-line intensity profiles about 5″ S of the galaxy center. In Hα, the secondary peak is about 30% as strong as the central peak. The [N II] λ6583 intensity profile is nearly identical to that of Hα.

Because the wavelength resolution is substantially less for this observation, the errors associated with the line widths are much larger. This accounts for the large scatter in Figure 6*b*. Nevertheless, there is a strong indication that the maximum line widths are in excess of 200 km s^{-1}, and that while the minimum widths are found well outside the center, the maximum width is offset approximately 2″ to the N of the nucleus. The rotation curve for NGC 2512 is fairly symmetric, with a maximum observed velocity amplitude of 260 km s^{-1}, or a deprojected amplitude of 300 km s^{-1}. The extrema are located 5″ from the center. There is an indication that the absolute value of the relative radial velocities continue to decrease at larger radii.

h) NGC 7316 (= Mrk 307)

This galaxy has a highly asymmetric, although nearly face-on disk with a prominent SE spiral arm. There is a distinct possibility that it has, or at one time had, an interacting companion because it is apparently enveloped by tidal debris. The central continuum and emission-line intensity profiles are very similar, with FWHMs of 5.″6 to 6.″2, or 1.6 to 1.7 h_{100}^{-1} kpc. The profiles are slightly steeper to the N of the nucleus than to the S. The Hα and [N II] λ6583 profiles, however, have a prominent secondary component 8″ to the S of center (approximately 35%–40% the strength of the central component), and weak component about 9″ to the N.

The FWHM of Hα are less than 100 km s^{-1}. The widths appear well behaved in that the maximum occurs in the center of the galaxy, and there is a general decline at larger radii. The velocity profile for NGC 7316 appears almost chaotic, with an amplitude of $\lesssim$10 km s^{-1}. This galaxy is nearly face-on, however, so its velocity profile provides the best evidence that the starburst is confined to a disk coaligned with the stellar disk. While we hesitate to point to significant trends in this rotation curve, the general decrease to the S of center in the galaxy is probably real, as are some of the bulk variations. The $I(\lambda 6716)/I(\lambda 6731)$ ratio for this galaxy is actually beyond the low-density limit for an electron temperature of 10^4 K: it is anomalous in this respect.

i) NGC 7714 (= Mrk 538)

NGC 7714, the SBG prototype (Weedman *et al.* 1981), is among the apparently brightest of this class of galaxies. It is interacting with a companion 1.′75 to the E, with a bridge between the two and a countertail in NGC 7714 itself. There are a number of large, nonstellar knots, loops, and dark lanes in the galaxy. The continuum and emission-line intensity profiles are fairly similar, with the same centers and similar widths: about 2.″5 to 2.″8, or 0.35 to 0.38 h_{100}^{-1} kpc. This makes NGC 7714 the most centrally condensed SBG in this sample in both the continuum and line emission. Still, both emission components are well resolved. There is a secondary intensity maximum approximately 3.″2 to the S in the galaxy which makes the profiles appear shallower in this direction.

The FWHMs of the emission lines vary between essentially zero well outside the nucleus, to a maximum of 180 km s^{-1} in the center, although the maximum widths are distinctly offset 2″ to the S of center. The structure in the Hα intensity profile is real. A discontinuous variation of the dispersion velocity of gas and stars in the nucleus of NGC 7714 (with several smaller scale features) probably indicates that the nucleus is not now in equilibrium. The rotation curve behaves similarly: there is a general trend to increase linearly from the center and ultimately flatten out, but the real structure in the curve once again probably betrays a settling down of the gas and stars into equilibrium with the gravitational potential of the nucleus. The maximum observed velocity amplitude is 190 km s^{-1}, or 220 km s^{-1} when corrected for inclination. NGC 7714 has the highest density in the S^+ volume, as indicated in Table 2.

V. DISCUSSION AND CONCLUSIONS

a) Comparison of SBG and AGN Properties

Having described the spatial and spectroscopic properties of the SBGs in our sample, we can now examine in detail their connection with AGNs. Perhaps the most striking result from this long-slit study is that the star formation is not confined to the centers of SBGs, but extends over many hundreds or even thousands of parsecs. Indeed, the center of the star-forming activity in some of these SBGs may not even be coincident with their galactic centers. It is possible, however, that the difference between the center of these SBGs (as defined by their emission-line rotation curves, assuming that these curves trace the underlying galaxy potential) and the continuum and line emission profile maxima may be due to large variations in reddening along different lines of sight near the nucleus. In either case, though, the intensity profile is markedly different from that in AGNs, where the profile is invariably strongly peaked at the center, and emission from the highest ionization lines is unresolved on the scale of an arcsecond.

The emission-line gas is almost certainly photoionized by nothing more exotic than O and B stars—the gas density in the S^+ emitting volume, and the level of ionization given by the $F([N\,II])/F(H\alpha)$ and $F([S\,II])/F(H\alpha)$ ratios, are both consistent with those found in giant H II region complexes (e.g., French 1980), although the line widths are often greater. Even very high ionization SBGs like Mrk 490C (De Robertis and Osterbrock 1986) are consistent with photoionization by a stellar continuum.

We note here that, without spatial information, published line widths and line profiles (e.g., Taniguchi 1987) may be erroneous. Because the effects of differential rotation over 2″ to 3″ can be substantial, line widths derived from one-dimensional detectors may be too large by more than 15%. In fact, line widths in these SBGs, with the possible exceptions of NGC 23 and NGC 1614, are distinctly smaller than those in AGNs. The individual line shapes, such as those published by

Taniguchi (1987), may be significantly skewed as well, either from rotational velocity shear or from patchy reddening in the nucleus. We listed the average asymmetry parameter, AI20 in Hα, for the central 1".6 for each galaxy in Table 2. (This value would roughly correspond to that published for SBGs based upon spectra obtained with one-dimensional detectors.) To illustrate the potential line profile skewing, we list AI20 as a function of slit position for three galaxies in Table 3. Clearly there are extreme variations in the profile shapes in all of the objects; in NGC 632 the asymmetry parameter even changes sign. Once again, this is entirely different from the AGN case where predominantly blueward profile asymmetries are probably due to differential extinction *and* radial cloud motion (see e.g., Whittle 1985), and the line shapes show no change across the (optically unresolved) nucleus.

It has never been suggested that SBGs must precisely match the optical properties of AGNs in order for a viable evolutionary link to exist. Still we are forced to reexamine what SBG properties motivated the suggestion of such a link. Balzano (1983) described a starburst galaxy as "... a spiral galaxy with a bright, blue nucleus which emits a strong, narrow emission-line spectrum similar to low-ionization H II region spectra. It may be undergoing an interaction with a nearby companion galaxy, and its nuclear near-infrared colors do not differ from normal galactic nuclei." Consequently, several candidates were rejected from her initial sample, chiefly ones in which the continuum and/or line emission was apparently not confined to the nucleus, based on the TV-guider image. Since we have found no SBG where the emission is confined to the nucleus (including the prototype, NGC 7714), based upon our higher quality spatial information, and, since we find no other close match (in ionization level, gas density, line width, or line profile) between SBGs and AGNs, we must reconsider the evolutionary connection.

b) *An Evolutionary Link between SBGs and AGNs?*

It is particularly tempting to speculate on the origin and evolution of SBGs and their possible relationship to AGNs. Balzano (1983) found that the space density of optically luminous SBGs is similar to that for classical Seyfert galaxies, suggesting that these phenomena may be related. In addition, she noted that about 30% of SBGs have companion galaxies, approximately the same ratio found for Seyfert galaxies by Dahari (1984). There is much circumstantial evidence suggesting that interactions may trigger the AGN phenomenon by disturbing the gravitational potential enough to allow a supply of gas to reach the central engine (e.g., De Robertis 1985), although the precise details remain unclear. In the same way, interactions in gas-rich galaxies might stimulate a gas flow into the nucleus, leading to the formation of a large number of massive stars through shocks and density enhancements. Gas not used up in star formation could then fuel the central supermassive compact object *if one exists*. Thus, one might anticipate that the evolutionary sequence would be from SBG to AGN simply because the gas must first be collected at the large scale and then funneled in toward the center. A typical period of revolution for a gas cloud situated a few hundred parsecs from the nucleus is $\sim 3 \times 10^7$ yr, in contrast to the lifetime of the starburst phase $\sim 2 \times 10^7$ yr (Weedman 1983). If these clouds require a few orbital periods (in a dissipative flow) to reach the central parsec, then the SBG and AGN phases should be well separated in time. On the other hand, if the interaction can supply enough gas at all radii simultaneously, then one would expect to see the AGN and SBG phases contemporaneously. That is, one would expect to see composite systems: optically luminous AGN/SBG galaxies. Although the question has not received much attention, there does not seem to be good evidence for the existence of such objects (e.g., Heckman *et al.* 1983). Because of the large differences in emission-line widths and levels of ionization between AGNs and SBGs (e.g., Veilleux and Osterbrock 1987; Balzano 1983), one might expect a substantial intermediate range in these features in composite objects. Such an intermediate range is rarely, if ever, observed (although NGC 23 might be a candidate), but rather the features are dominated by one extreme or the other.

The evolutionary sequence might proceed in the opposite direction, however. The active nucleus could influence the star formation history of the disk via strong outflowing winds which would interact with the interstellar gas on up to kiloparsec scales, leading to a burst of star formation and perhaps choking its gas supply at the same time. In this picture the starburst phase would be more-or-less contemporaneous with the AGN phase if the AGN lifetime is greater than 10^6 yr, while the characteristic wind or narrow-line cloud crossing time scales are less than $10^{6.5}$ yr. Indeed, bursts of star formation sometimes accompany an active nucleus: De Robertis and Pogge (1986) and Wilson *et al.* (1986) have found evidence for bursts of star formation in the nuclei of some Seyferts. In particular, there are several massive H II complexes in the center of the Seyfert 1 galaxy NGC 7469 which, by themselves, would constitute a low-luminosity SBG. But the integrated Hα flux from these massive H II regions is orders of magnitude less than the combined flux from the broad- and narrow-line Hα regions. In addition, classical Seyfert 2 galaxies have median Hα luminosities $\sim 10^{41}$ ergs s^{-1} (Dahari and De Robertis 1988), which are quite comparable to those for SBGs, $\sim 10^{40.5}$ ergs s^{-1} (Balzano 1983). Thus the integrity of the Seyferts remains intact: bursts of star formation, when they accompany the AGN phase, do not seem to dominate the emission-line flux.

A more detailed model outlining the evolution of a SBG into an AGN has been described by Weedman (1983). Assuming a typical dimension for the nuclear starburst volume of 100 pc, he found that the cluster of massive-star remnants (black holes), originally not in equilibrium with the bulge potential, could collapse to a steady state configuration which is considerably more centrally condensed. When a sufficient number of black holes is contained within ~ 1 pc, and *if* there is a sufficient supply of gas, the AGN phase begins. His arguments are also based on the assumption that the kinematics of the starburst are decoupled from the Population II stars. This assumption is based on the work of Feldman *et al.* (1982), who found the average radial velocity dispersion, σ, of a number of SBGs (based on the width of λ5007) to be approximately 70 km s^{-1}. (The widths reported by Feldman *et al.* are, if anything, slightly too large because they undoubtedly contain a galactic rotational component, as our long-slit data demonstrates. The mean dispersion of our sample is of this same order, however.) Both Weedman (1983) and Balzano (1983) have argued that since the mean velocity dispersion for the bulges of spiral galaxies (e.g., Whitmore and Kirshner 1981) is well over twice that of the emission-line material, and since the SBGs apparently follow the extrapolation of the $L \propto \sigma^4$ relation found for H II complexes by Terlevich and Melnick (1981), then one could consider the starburst nucleus as a single (giant)

H II complex which is simply not yet in equilibrium with the potential of the underlying galaxy. There is no *a priori* explanation for the large difference in the velocity dispersion between the two populations. Indeed, it is difficult to conceive of any plausible scenario which would produce two populations with such radically different dispersion velocities.

The major difficulty with Weedman's two-phase model is that the observed characteristic starburst dimension is clearly several times larger than he assumed in his calculation, so that equipartition *can* be achieved between the gas and older stellar populations without a substantial collapse from the young stellar remnants. Furthermore, we consider it more likely that the H II complexes which comprise the starburst are rotationally supported and are contained within a disk- or pillbox-shaped volume, roughly coplanar with the large-scale stellar disk. The most compelling argument for this hypothesis is given by the series of velocity curves displayed in part *c* of Figures 1–9. All of the galaxies have projected velocity curves which describe reasonably well-behaved rotating systems like those observed in disk galaxies: rising linearly with distance outside the nucleus and flattening off hundreds of parsecs from the center. Such behavior is not expected in an isothermal distribution like that envisioned in the two-phase model. Further, the velocity curve for the face-on galaxy NGC 7316, with a velocity amplitude of only 20 to 30 km s^{-1}, provides compelling evidence that the disk of gas and stars participating in the starburst must be nearly coaligned with the galactic disk. The observed line widths for the SBGs in our sample also support our H II disk model. The widths, which range from 80 to 220 km s^{-1}, are a combination of the intrinsic velocity dispersion in the disk convolved with a rotational component, with a small line-of-sight component as well. Approximate dispersion velocities out of the plane of the disks span a (reasonable) range of 30 to 90 km s^{-1}. Data for a few slit orientations for each object should be acquired and analyzed in a manner similar to De Robertis and Pogge (1986) to confirm our view.

The total mass in stars associated with a luminous starburst is given by Weedman (1983) as $\sim 10^{-41} L(\mathrm{H}\alpha) T_{sb}\ M_\odot$, where $L(\mathrm{H}\alpha)$ is the Hα luminosity (ergs s^{-1}) and T_{sb} is the duration (yr) of the starburst. For stars of 5–10 $M_\odot$, the lower limit to the lifetime of the starburst phase is 2×10^7 yr (Weedman 1983). Thus, a total mass of 10^7–10^8 $M_\odot$ may be tied up in star formation over this short period given a SBG median Hα luminosity (Balzano 1983) of $\sim 10^{40.5}$ ergs s^{-1}. If confined to a disk, then one would expect a number of giant H II regions rather than a single massive complex (e.g., Weedman 1983). The Hα luminosities of the largest H II complexes in nearby spirals (e.g., Searle 1971) are about 10^{39} ergs s^{-1}. Thus, the optically luminous SBGs are probably made up of many tens to thousands of such massive complexes. In this case, one would expect the Hα intensity profiles (part *a* of Figs. 1–9) to be fairly smooth with only some low-level secondary structure. This is indeed what is observed. High-quality, high-resolution imaging of these nuclei will be required to investigate this problem further, although optical studies could be severely hampered by dust and gas which may shroud much of the disk and the individual H II complexes.

c) *Conclusions*

In summary, we have found from long-slit spectroscopy of nine optically luminous SBGs that star formation is not confined to their nuclei, but extends up to kiloparsecs from their centers. This extended emission, coupled with their narrow line widths and low ionization, distinguish SBGs from AGNs morphologically and spectroscopically. Our rotation curves and velocity profiles both suggest that the star formation occurs in a large, disk-shaped volume which is supported by rotation, and contains from tens to thousands of separate, massive H II region complexes. Given the large spatial extent of the star formation, and its disk environment, it is difficult to see how an evolutionary link between SBGs and AGNs could operate.

This work was supported in part by NSF grants AST 83-11585 and AST 86-11457 to the University of California, under the direction of D. E. Osterbrock, and by the Natural Sciences and Engineering Research Council of Canada. We thank Dr. Osterbrock for his useful comments and encouragement for this project, as well as R. Pogge and S. Veilleux for helpful comments. Support for the Lick Observatory hardware and data reduction software was provided through NSF grant AST 86-14510.

REFERENCES

Balzano, V. 1983, *Ap. J.*, **268**, 602.
Dahari, O. 1984, *A.J.*, **89**, 966.
Dahari, O., and De Robertis, M. M. 1988, *Ap. J. Suppl.*, **67**, in press.
De Robertis, M. M. 1985, *A.J.*, **90**, 1343.
De Robertis, M. M., and Osterbrock, D. E. 1986, *Pub. A.S.P.*, **98**, 629.
De Robertis, M. M., and Pogge, R. W. 1986, *A.J.*, **91**, 1026.
de Vaucouleurs, G., de Vaucouleurs, A., and Corwin, H. G., Jr. 1976, *Second Reference Catalogue of Bright Galaxies* (Austin: University of Texas Press).
Evans, I. N., and Dopita, M. A. 1985, *Ap. J. Suppl.*, **58**, 125.
Feldman, F. R., Weedman, D. W., Balzano, V. A., and Ramsey, L. W. 1982, *Ap. J.*, **256**, 427.
French, H. B. 1980, *Ap. J.*, **240**, 41.
Heckman, T. M., Miley, G. K., van Bruegel, W. J. M., and Butcher, H. R. 1981, *Ap. J.*, **247**, 403.
Heckman, T. M., van Breugel, W. J. M., Miley, G. K., and Butcher, H. R. 1983, *A.J.*, **88**, 1077.
Lauer, T. R., Miller, J. S., Osborne, C. S., Robinson, L. B., and Stover, R. J. 1984, *Proc. SPIE*, **445**, 132.
Phillips, M. M., Charles, P. A., and Baldwin, J. A. 1983, *Ap. J.*, **266**, 485.
Pogge, R. W., and Eskridge, P. B. 1987, *A.J.*, **92**, 291.
Pritchet, C. J. 1977, *Ap. J. Suppl.*, **37**, 397.
Sandage, A. 1961, *The Hubble Atlas of Galaxies* (Washington, DC: Carnegie Institution).
Searle, L. 1971, *Ap. J.*, **168**, 327.
Shuder, J. M., and Osterbrock, D. E. 1981, *Ap. J.*, **250**, 55.
Taniguchi, Y. 1987, *Ap. J. (Letters)*, **317**, L57.
Telesco, G. M., Becklin, E. E., Wynn-Williams, C. G., and Harper, D. A. 1984, *Ap. J.*, **282**, 427.
Terlevich, R., and Melnick, J. 1981, *M.N.R.A.S.*, **195**, 839.
Veilleux, S., and Osterbrock, D. E. 1987, *Ap. J. Suppl.*, **63**, 295.
Weedman, D. W. 1983, *Ap. J.*, **266**, 479.
Weedman, D. W., Feldman, F. R., Balzano, V. A., and Ramsey, L. W. 1983, *Ap. J.*, **256**, 427.
Weedman, D. W., Feldman, F. R., Balzano, V. A., Ramsey, L. W., Sramek, R. A., and Wu, C.-C. 1981, *Ap. J.*, **248**, 105.
Whitmore, B. C., and Kirshner, R. P. 1981, *Ap. J.*, **250**, 43.
Whittle, M. 1985, *Ap. J.*, **213**, 1.
Wilson, A. S., Baldwin, J. A., Sun, S.-D., and Wright, A. E. 1986, *Ap. J.*, **310**, 121.

MICHAEL M. DE ROBERTIS: Department of Physics, York University, 4700 Keele St., North York, Ontario M3J 1P3, Canada

RICHARD A. SHAW: Lick Observatory, University of California, Santa Cruz, CA 95064